Chapter 2

The Molecular Survey

Previous molecular investigations of Ae/Be stars (Loren 1975; Canto, *et al.* 1984; Levreault 1988) were directed towards establishing the association of molecular gas with the young stars and searching for evidence of molecular outflows. The conclusions of these studies were that small (0.5-2 pc), sometimes multiply peaked CO clouds are seen towards all Ae and Be stars associated with nebulosity, although in many cases the peaks are offset from the stars. Gas morphology and kinematics arguments, namely that the velocity dispersions are highest at the positions of the central stars and decrease dramatically at positions away from these peaks, were used to suggest that the molecular emission is indeed physically associated with the young high mass stars. Loren (1975) even argued that the observed velocity widths as a function of radial distance from the star implied actual cloud collapse in several cases, although simple turbulence was sufficient in most cases.

Our molecular survey provides data of higher spatial resolution by 50-350% (depending on the region) compared to those mentioned above, and was designed as a first order "snapshot" exploration of the basic cloud core properties in isolated regions forming Ae/Be stars. In all cases our molecular maps cover a region much larger than the anticipated size of the local star-forming site. We use ^{12}CO to determine the extent and structure of the optically thick molecular gas, to derive characteristic core temperatures, and to identify outflow sources. We use ^{13}CO in combination with ^{12}CO, relying upon simple LTE analysis, to determine the gas column density as a function of position, and to derive gas masses. In anticipation that in some cases ^{13}CO might be optically thick we also obtained C^{18}O in order to trace optically thin gas; this line is certain not to be optically thick under the typical conditions expected for clouds in which star formation is already taking place. From observations of CS we trace the structure of the dense gas.

2.1 Observations and Data Reduction

Molecular data in the ^{12}CO (J=1-0), ^{13}CO (J=1-0), C^{18}O (J=1-0), and CS (J=2-1) transitions were obtained by LAH with the Five College Radio Astronomy Observatory 14m telescope and QUARRY receiver array in 1993 April and in 1993 September. The spectrometer consists of two 32-channel filter banks which provide data simultaneously at 1.6 and 6.4 km s^{-1} resolution (assuming 2.5 channels per resolution element). The telescope half-power beam width is 45 arcsec at 2.6 mm and the main beam efficiency is 0.54 when the source fills the beam (the situation we have assumed in our observations of cores containing Ae/Be stars). The array is capable of mapping a 4.2 arcmin $\times$ 5.0 arcmin area in two pointings with positional uncertainties in the absolute pointing of about 5-7 arcsec rms. Our observations were single-beam spaced (every 50 arcsec) in CO while in CS they were half-beam spaced, and the total areal coverage is 8.4 $\times$ 10.1 arcmin in ^{12}CO , ^{13}CO , and CS, and 4.2 $\times$ 5.0 arcmin in C^{18}O .

Absolute position-switching was used, with the telescope alternating between the on-source position and a nearby off-source positon established during the observations to be free of CO. Except at C^{18}O where the references were not shared, at each position typically two on-source measurements of 10 seconds integration were made for every one off-source measurement of 20 seconds integration. Total on-source integration times per pixel were 40 (^{12}CO), 150 (^{13}CO), 50 (CS) , and 300 (C^{18}O) seconds. The data were corrected for the off-line reference level by subtracting a linear baseline constructed from the average flux over the V_{lsr} intervals representing line-free regions of the spectrum.

2.2 Analysis

We summarize in Table 2.1 the results on CO and CS characteristics in the vicinity of the young, massive, isolated Ae/Be stars in our sample. This list is ordered by decreasing Ae/Be mass, and constitutes the complete set of stars on which we base our study. We do not possess molecular data ourselves for 3 of the regions in this Table (RR Tau, LK Hα 218, and LK Hα 233), but do report information from the literature where it is available. The CO line structure and two-dimensional morphology is qualitatively described. Linewidths and antenna temperatures are also given. We begin our discussion by describing the molecular gas distributions as traced via column density, then estimate cloud core masses and radii, and finally, briefly mention the kinematic information that exists in our data (although we do not rigorously investigate kinematic issues).

2.2.1 Core Morphology from Column Density and Dense Gas Maps

From our FCRAO observations we confirm the general morphological statements made previously in the literature, namely, that the cloud cores associated with Ae/Be stars are typically small in extent and that the stars themselves are not necessarily located at the molecular peaks. However, we now wish to clarify these impressions by projecting molecular column density and optical maps upon one another.

In order to compute the line-of-sight opacity through the cloud, we have performed a simple LTE analysis following Dickman (1978) with the standard assumptions that ^{12}CO is optically thick while ^{13}CO is optically thin. These assumptions seem reasonable given 1) the ratio of ^{12}CO to ^{13}CO antenna

Table 2.1. Summary of Parameters Derived from Molecular Data

Ae/Be Star (1)	Mass $M_\odot$ (2)	CO Velocity Structure (3)	2-D Extinct. Morphology (4)	Δv ^{12}CO (5)	T_A^* ^{12}CO (6)	T_A^* ^{13}CO (7)	T_A^* $C^{18}O$ (8)	A_V mag (9)	M_{total} $M_\odot$ (10)	size pc (11)	CS Detect.? (12)
MWC 297	26.5	mult. components	PDR?	4.0	2.2	1.2	0.20	11	1500:	–	–
MWC 1080	20.6	outflow + self absorb.	spherical	14.1	4.4	2.0	n.d.	22	1406	1.1	yes
MWC 137	18.9	outflow?	PDR?	6.1	4.6	0.6	n.d.	3	83:	–	–
BD +40° 4124	12.6	mult. components	cometary	3.9	14.2	5.4	0.65	50	862	0.7	yes
Lκ Hα 198	9.6	outflow	mult. peak	3.9	7.2	2.7	–	18	373	0.4	–
Lκ Hα 215	9.5	outflow?	edge of cloud	3.8	6.8	1.7	0.15	9	312	0.5	–
HD 259431	8.9	velocity gradient	edge of cloud	2.7	9.5	3.0	–	19	480	0.8	–
Lκ Hα 234	8.5	outflow	compressed	5.5	9.5	4.8	0.65	40	1860	1.5	yes
RR Tau*	8.4	–	star at peak	1.8	12.3	2.2	–	2	240	1.6	–
VV Ser	7.5	flat-topped lines	uniform distrib.	6.2	1.4	1.0	n.d.	13	–	–	–
BD +46° 3471	7.3	outflow	mult. peak	2.6	6.5	2.5	0.20	8	259	0.7	yes
HD 200775	7.2	mult. components	PDR	3 or 7	2.8	0.4	0.30	2	717:	–	yes
BD +61° 154	5.1	velocity gradient	small cloud	3.9	4.3	1.2	n.d.	7	<180	0.2	–
Lκ Hα 208	4.1	mult components	ridge of emission	2.7	4.8	1.9	–	8	638	–	–
HD 250550	3.9	mild vel. gradient	mult. peak	2.9	3.6	1.2	–	6	140	0.5	–
Lκ Hα 218	3.8	–	–	–	–	–	–	–	–	–	–
Lκ Hα 233*	2.6	velocity gradient	star at edge	1.6	14.3	4.5	–	6	250	1.0	–

* Entries for Lκ Hα 233 and RR Tau are taken from Loren (1975).

Column (2): Stellar mass repeated from Table 1.1
Column (3): Qualitative description of CO line profile
Column (4): Qualitative description of CO spatial structure; "PDR" denotes candidate photodissociation region
Columns (5-9): Δv, T_A^*, and A_V values at the positions of the Ae/Be stars (may be different elsewhere);
"n.d." in Column (7) means $C^{18}O$ is not detected
Column (10): $M_{total} = M_H + M_{He} = 1.36 M_H = 1.36 \times 2 m_H (N_{H_2}/cm^{-2})(A/cm^2)$ integrated over entire molecular image
Column (11): Cloud sizes determined from FWHM measurements of column density maps; not given in cases of PDR's or uniform gas distributions
Column (12): Notation of CS detection is positive if dense gas appears anywhere in the 8.4×10.0 arcmin field

temperatures which, in all cases, is less than the optically thin abundance ratio of 50-60 (Langer & Penzias 1990); 2) the ratio of ^{13}CO to C^{18}O antenna temperatures which, in all cases where both are available, is greater than the terrestrial abundance ratio of 5.5 (although this assertion seems to apply only for extinction values $A_V < 10 - 20$ according to Bachiller & Cernicharo, 1986); 3) the accuracy to which the ^{13}CO and C^{18}O contours trace one another; 4) the computed LTE values of $\tau(^{13}\mathrm{CO}\ ) \lesssim 0.5$. We take the relationship between core extinction and hydrogen column density to be $A_V = N(H_2)\ /\ 1 \times 10^{21}$, where $\mathrm{N}(H_2) = \mathrm{N}(^{13}\mathrm{CO}\ )/2 \times 10^{-6}$. Beam-averaged molecular extinction values *at the positions of the stars* are reported in Table 2.1. These numbers range from 2-50 mag and are uncertain at the 20-50% level.

We show the column density maps in Figure 2.1 superposed on I-band CCD images (described in Chaper 3) for 12 of the 14 Ae/Be regions for which we have molecular data. Contours begin at A_V =5 mag and increase in 5 mag intervals. We do not show the remaining 2 regions (LK Hα 208 and VV Ser). In the case of LK Hα 208, the column density map consists of a single 5 mag contour running north-south through the position of the star. In the case of VV Ser, the ^{12}CO and ^{13}CO temperatures are comparable and the line profiles flat-topped; thus, we do not trust the column density information derived from LTE analysis. As can be seen from Figure 2.1 (see Table 1.1 for the translation from arcmin to pc for each region), the peak core extinction is typically not coincident with the Ae/Be star, but is offset from it by several tenths of a pc. We conclude that the Ae/Be stars are located near the edges of the small clouds with which they are associated and, in many cases, in the midst of steep column density gradients. Within our sample, only HD259431 is found near the actual peak of the molecular emission.

To generalize, instead of spherically symmetric molecular cores centered at the positions of the stars, the local low-density gas distributions often have

Figure 2.1. *Molecular column density maps for 12 Ae/Be regions.* These images are 8.4×10.1 arcmin in size, and consist of contoured extinction maps based on data obtained with the QUARRY array receiver at the Five College Radio Astronomy Observatory superposed on I-band CCD images obtained with the T2KA CCD and 0.9m telescope at the Kitt Peak National Observatory. See Table 1.1 for the translation from arcmin to pc for each region. Of our full sample of 17 Ae/Be regions, we have molecular data for 14; of these 14 we show only 12 in this Figure (see text). The maps are organized in order of decreasing Ae/Be mass (from top to bottom and left to right). Individual maps are centered on the Ae/Be stars themselves with contours beginning at $A_{\rm V} = 5$ mag and increasing in 5 mag intervals in every case. Molecular extinction values at the positions of the stars range from 2-50 mag (see Table 2.1). We note that in most cases the molecular gas distributions are neither spherically symmetric nor centrally peaked on the Ae/Be stars.

MWC 297

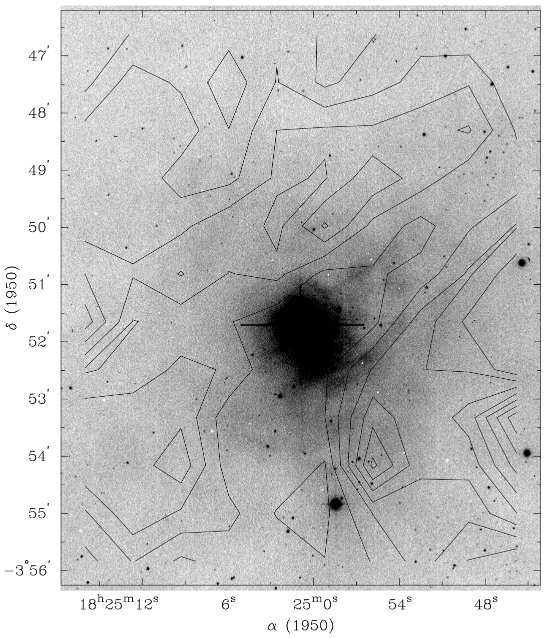

MWC 137

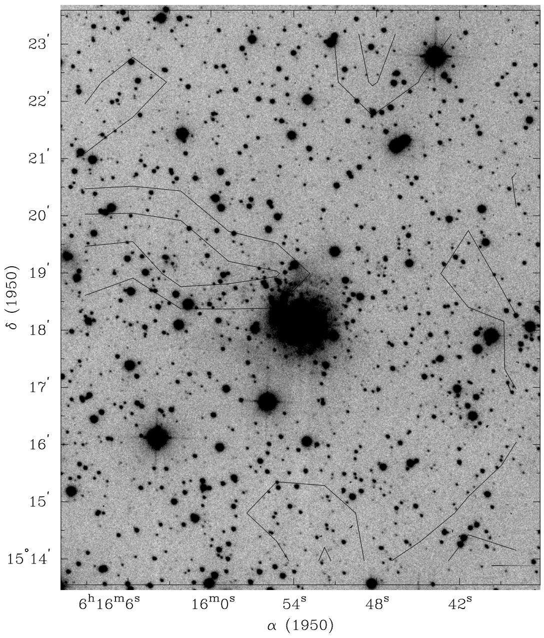

MWC 1080

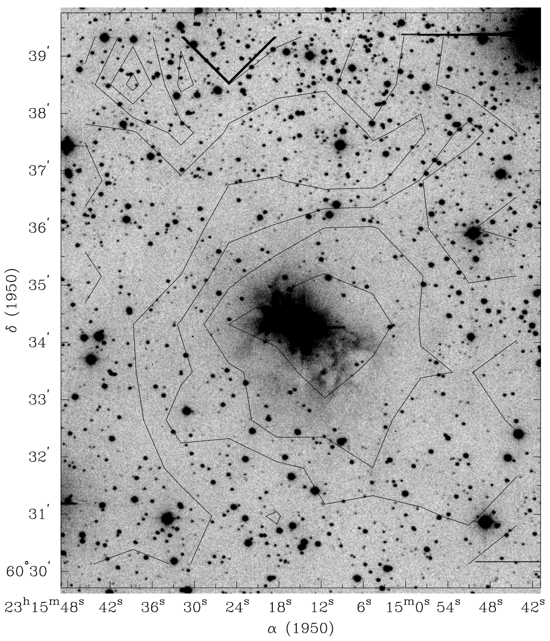

BD+40 4124

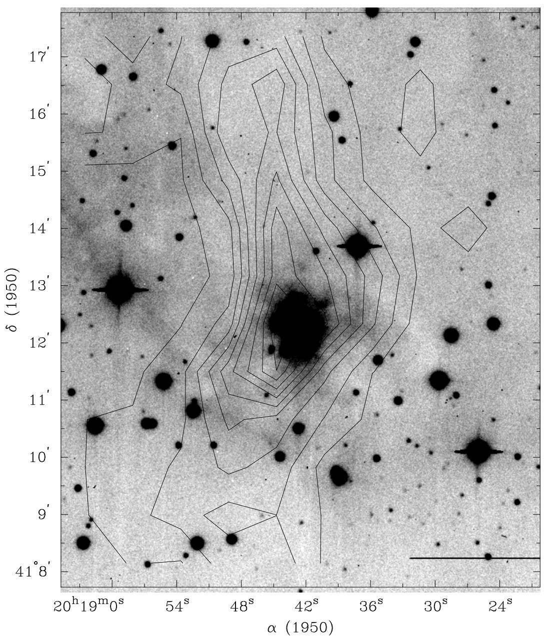

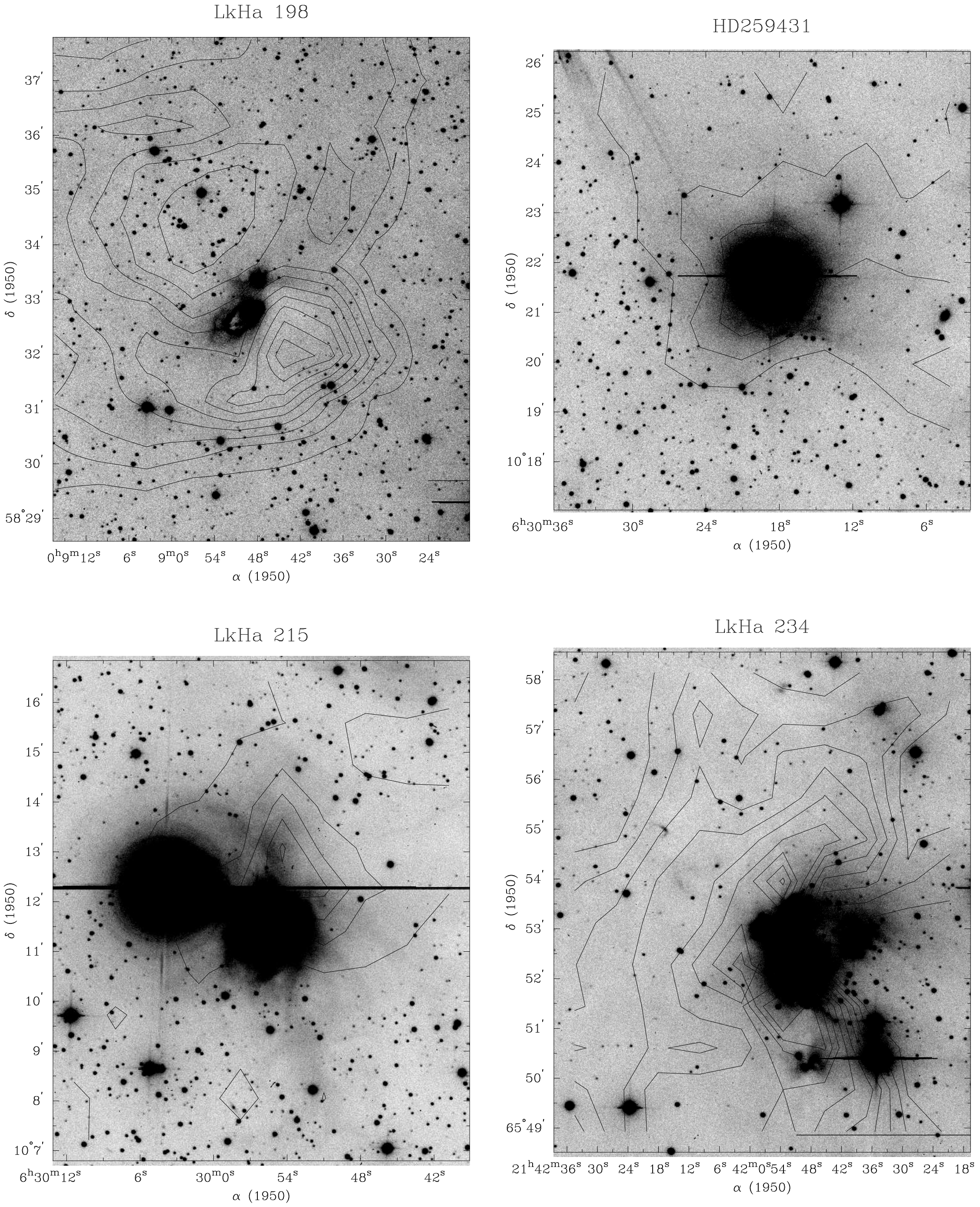
LkHa 198
δ (1950)
37′
36′
35′
34′
33′
32′
31′
30′
58°29′
0h9m12s 6s 9m0s 54s 48s 42s 36s 30s 24s
α (1950)
HD259431
δ (1950)
26′
25′
24′
23′
22′
21′
20′
19′
10°18′
6h30m36s 30s 24s 18s 12s 6s
α (1950)
LkHa 215
δ (1950)
16′
15′
14′
13′
12′
11′
10′
9′
8′
10°7′
6h30m12s 6s 30m0s 54s 48s 42s
α (1950)
LkHa 234
δ (1950)
58′
57′
56′
55′
54′
53′
52′
51′
50′
65°49′
21h42m36s 30s 24s 18s 12s 6s 42m0s 54s 48s 42s 36s 30s 24s 18s
α (1950)

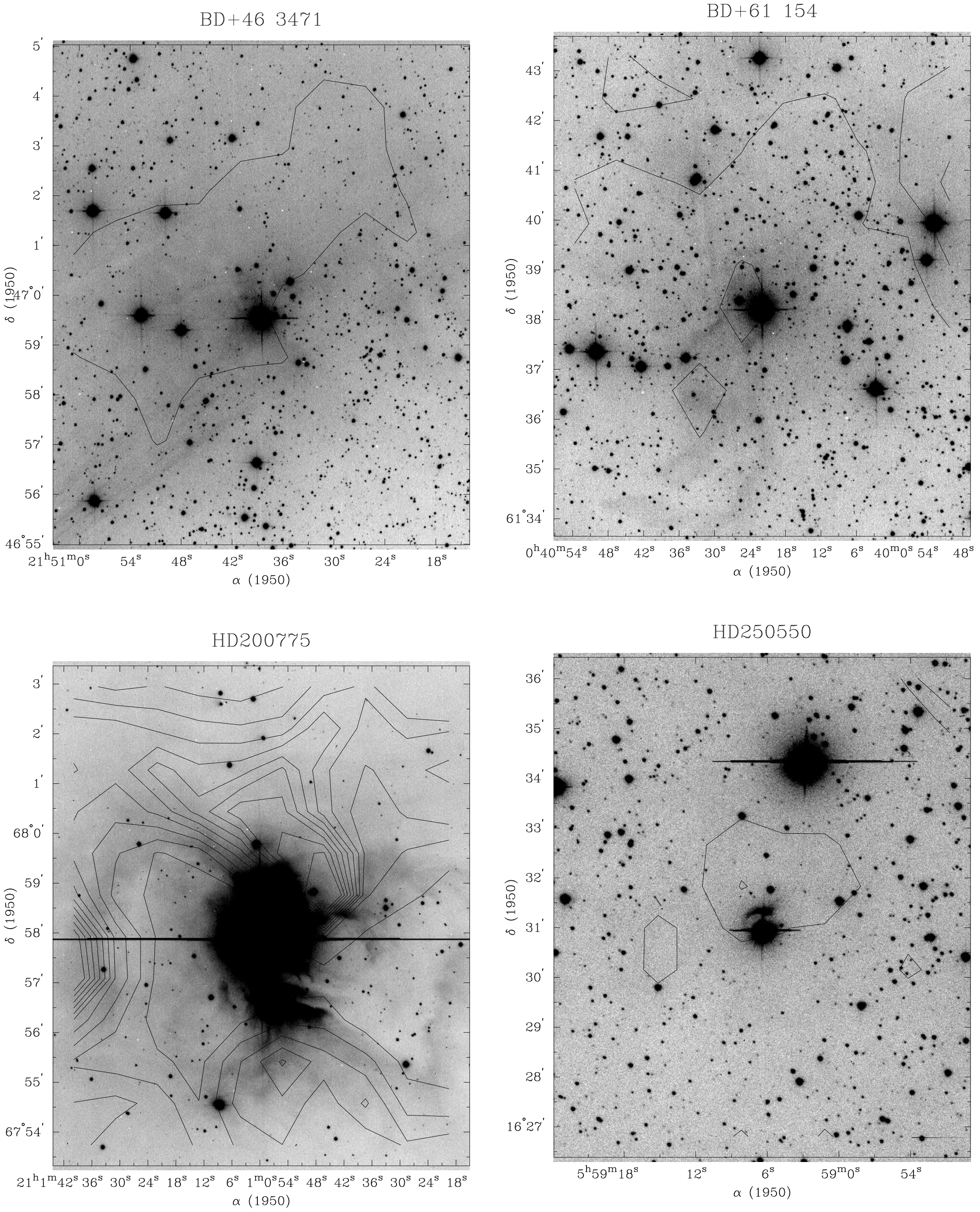
BD+46 3471
δ (1950)
α (1950)
BD+61 154
δ (1950)
α (1950)
HD200775
δ (1950)
α (1950)
HD250550
δ (1950)
α (1950)

morphologies which appear cometary, asymmetrically compressed, or otherwise disturbed. The implication is that the clouds are not undergoing quiescent collapse and/or fragmentation, but have been disrupted in some manner. We speculate on two possible scenarios. Either:

- The clouds have been subject to external dynamical processes which have altered the protostellar cores. In the radiative-driven implosion picture of star formation (Bertoldi *et al.* 1993, Elmegreen 1992), compression of a molecular cloud clump by ionizing radiation or an external shock can aid in, or even induce, the formation of massive stars.

or

- The stars themselves have created the observed column density gradients by dissociating significant amounts of molecular material via heating of circumstellar dust and subsequently gas (via gas-grain collisions). Early OB stars in molecular cores will create hydrogen photodissociation regions several tenths of a pc to several pc in size (Roger & Dewdney 1992), dependent upon the ambient cloud density. Thus, in most cases we can consider our extinction maps as lower limits only. We note that there is some evidence for the infusion of energy into the clouds by the stars, based on the observation of collimated jets (Corcoran *et al.* 1994, Ray, *et al.* 1990, and Poetzel *et al.* 1992 for LK Hα 198, LK Hα 234, and MWC 1080 respectively) and molecular outflows (see below and Levreault 1988) in several cases.

We would like to explore further this speculation that the Ae/Be stars are located near the edges of their parent cores. We have already noted that in two dimensions, projected on the sky, the stars do not define the geometrical centers of the clouds. As for the third dimension, we can use obscuration as a surrogate spatial measure if the core is non-clumpy and if photodissociation is unimportant. Following Loren (1975), we plot in Figure 2.2 the line-of-sight extinction towards the Ae/Be star (computed from optical spectroscopic and photometric information, as given in Table 1.1) corrected by the canonical interstellar extinction between the sun and the molecular cloud (0.9 mag/kpc), against the extinction computed from the beam-averaged molecular column density, as given in Table 2.1. Interpreted literally, this diagram implies that the Ae/Be stars are typically seen through less than 50% of the total molecular column density. Combined with the evidence from our extinction maps that the stars are near the edges of the clouds, that the stars also appear to be near the fronts of the clouds, strengthens our suggestion above that there may be some dynamical interaction occuring either before or after the star formation process, between the stars and their environments.

What about dense gas? In cases where measurements were made of CS, we have indicated its presence or absence in Table 2.1. The results on the CS core morphologies are qualitatively the same as those derived from our CO data. There is a definite absence of dense gas *at* the positions of Ae/Be stars; instead, high-density ridges or globules are typically found to be offset by more than 0.1 pc from the massive stars. These results are not dissimilar to those found by Myers *et al.* (1987) and Benson & Myers (1989) in a survey of NH_3 cores associated with high-mass stars.

2.2.2 Cloud Size and Mass Estimates

In this section we use our column density maps to obtain estimates for the macroscopic parameters of the cloud cores associated with Ae/Be stars.

The cloud sizes reported in Table 2.1 were derived by estimating, where possible, the radially averaged full-width - half-max values of the peaks in the column density maps. These numbers are highly uncertain due both to ambiguity

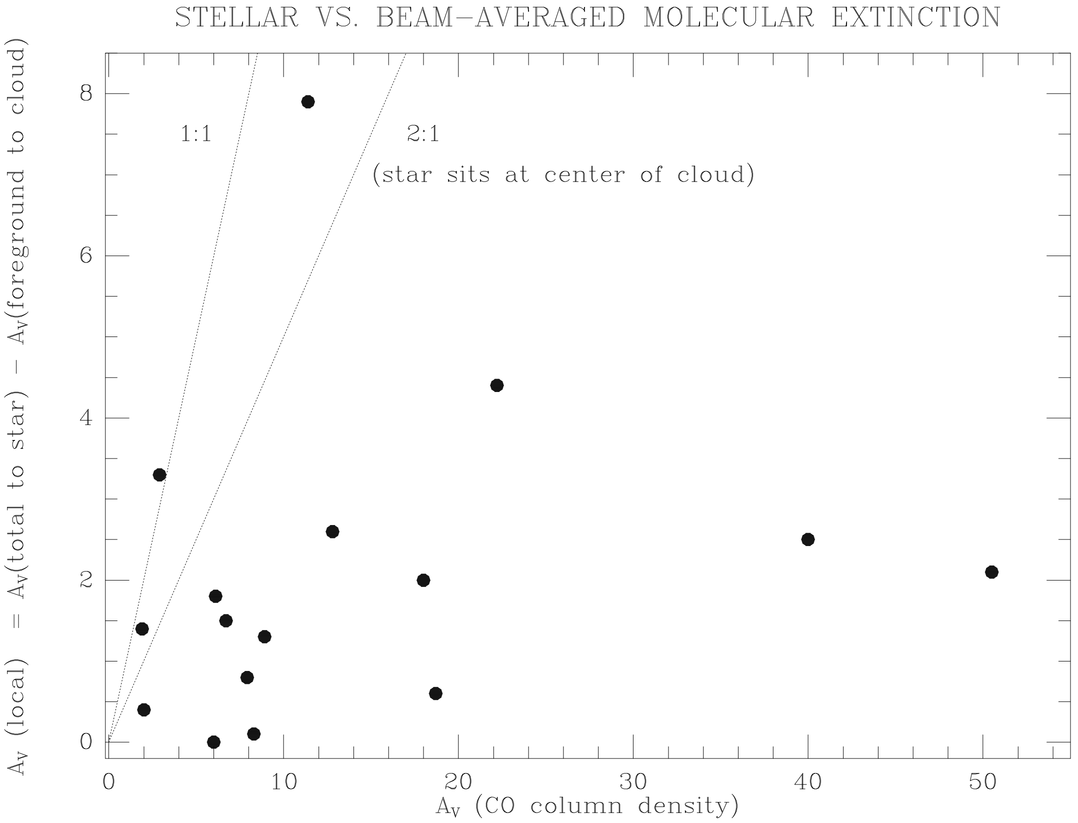

Figure 2.2. *Local interstellar / circumstellar extinction towards Ae/Be stars versus beam-averaged molecular extinction.* Local extinction is computed by subtracting the canonical interstellar extinction between the sun and the molecular cloud (0.9 mag/kpc) from the stellar extinction determined from optical spectroscopic and photometric information. Molecular extinction is computed from the LTE analysis. If extinction can be used as a surrogate for depth or distance, we typically find the Ae/Be stars to be located on the near sides of the clouds.

in the definition of a cloud "core" and to the non-symmetric gas morphologies. We intend them only as approximate guides to the physical extent of these spatially isolated star-forming sites. For the Ae/Be cores in our sample, the range in cloud radii is from about 0.1-0.8 pc, consistent with or slightly larger than the canonical definition of a cloud core.

The cloud masses reported in Table 2.1 were estimated using

$$M/M_{\odot} = M_H/M_{\odot} + M_{He}/M_{\odot} = 1.36\ M_H/M_{\odot}$$

where

$$M_H/M_{\odot} = 2(m_H/M_{\odot})(N_{H_2}/cm^{-2})(A/cm^2).$$

N_{H_2} and A are summed from our column density maps over all pixels in which emission is detected. For the Ae/Be cores in our sample, the range in cloud masses is from about $150 - 2000$ $\mathrm{M}_{\odot}$, consistent with what is found (*cf.* by Loren, 1978) in other cores producing intermediate-mass stars, *e. g.* the R CrA cloud (650 $\mathrm{M}_{\odot}$) or the ρ Oph cloud (1800 $\mathrm{M}_{\odot}$). We caution, however, that the peculiar cloud morphologies could affect our ability to accurately determine gas masses.

2.2.3 Gas Kinematics from CO Line Profiles

In this section we briefly discuss the velocity information available from our molecular data cubes, although we do not undertake a rigorous analysis of the kinematic properties of the Ae/Be clouds. We employ both position-velocity maps and by-eye examination of the line profiles. As a general statement, the velocity structure of the Ae/Be clouds is as rich in complexity as is the two-dimensional morphological structure. A summary of our findings for individual sources on ^{12}CO line widths and line structure can be found in Table 2.1.

Evidence for outflows (bi-polar or uni-polar high-velocity CO wings) is seen in the cases of BD+46 3471, HD 250550 (weak), LK Hα 198, LK Hα 215 (weak), LK Hα 234, MWC 137 (weak), and MWC 1080. Of these, LK Hα 215 and MWC 137 appear to be new detections based on their absence from the lists of Fukui (1991 or 1989). Inspection of CO(2-1) data, a better outflow indicator than the optically thick CO(1-0) transition used here, for these regions would be prudent in order to confirm our claims. We find the apparent outflow detection rate (7 of our 14 sources) remarkable given the optically visible nature of these sources. However, we note that our data have not proven the outflows to be associated with the Ae/Be stars themselves, only that they are located within approximately 30 arcsec of the Ae/Be stars. We will present evidence in the form of infrared imaging in Chapter 5 showing, in fact, that there are many potential candidate outflow sources among the significant embedded populations found over this size scale.

Other interesting velocity structures are also clearly seen in our data, including uniform velocity gradients, and arcs and "holes" in position-velocity space. We encourage the undertaking of higher-spectral resolution observations in order to properly probe the dynamics of the Ae/Be cores, and conclude only that simplistic pictures involving spherical clouds collapsing in isolation to produce massive stars, do not seem to justified from our data.

2.3 Conclusions from the Molecular Survey

Our FCRAO survey has provided us with a crude picture of the distribution and kinematics of molecular gas in isolated cores containing young, high-mass Ae/Be stars. From our column density maps we have determined characteristic cloud sizes (0.1-0.8 pc) and masses ($150 - 2000$ $M_{\odot}$), and find that they are generally consistent with those typical of star forming cores in which high-mass stars are being produced (*cf.* Myers *et al.* 1987). Also, we have identified two new candidate outflow sources and two candidate photodissociation regions; these are indicated in Table 2.1. We note in passing that there are no relationships between the mass of the Ae/Be star and the mass of the cloud, the line-of-sight column density, or the core morphology (*n.b.* Table 2.1 is presented in order of decreasing Ae/Be mass).

We originally intended to use this data to compare the opacity of the clouds with the derived extinction values towards individual young stars projected onto the clouds (see Chapter 5). Our goal was to estimate which stars in the local groups surrounding the Ae/Be stars might not be physically associated with the central massive star, but instead could be background stars seen through the less opaque outer portions of the cloud. We have learned instead, however, that the molecular cores containing Ae/Be stars are typically asymmetric structures with large column density gradients (several tens of magnitudes in some cases) near the positions of the central massive stars. We have suggested this as evidence for interaction between the stars and the cores – with the ambient clouds being disrupted due either to external dynamical processes or to internal (from stellar photons) molecular dissociation. We offer the caveat, however, that higher-spatial and higher-spectral observations are required in order to probe morphological and dynamical issues with any further accuracy.